Reports

Geometry, Topology, and Universality of Random Surfaces

JAYANATH R. BANAVAR, AMOS MARITAN,* ATTILIO STELLA

Previous simulations of a self-avoiding, closed random surface with restricted topology (without handles) on a three-dimensional lattice have shown that its behavior on long length scales is consistent with that of a branched-polymer. It is shown analytically that such a surface with an unrestricted number of handles has a qualitatively different geometry and therefore is in a different universality class. The effect of a net external pressure is to suppress the handles and collapse the surface into a branched polymer–like configuration. Topology is thus shown to be a key factor in determining the universality class of the system.

RANDOM SURFACES PLAY AN IMPORTANT role in diverse areas such as biology (red blood cells, the lungs), (*1*) material science (crystal growth, microemulsions, aerogels) (*1*), and high energy physics (quark confinement, string theories) (*2*). For instance, a three-dimensional vesicle can be modeled as a self-avoiding, closed random surface with otherwise arbitrary topology (an unrestricted number of handles) enclosing a connected volume (*3*). The topology of a surface may be characterized in terms of the Euler characteristic $\chi = 1/2\pi \int ds\, K$ where the integral is over the surface and K is the Gaussian curvature (*3*). χ is related to the number of handles H by $\chi = 2 - 2H$ and is a topological invariant under deformation of the surface (Fig. 1). The geometry of a vesicle may be described by two exponents d_S and d_V defined by $S \sim R^{d_S}$ and $V \sim R^{d_V}$ where S, V, and R are the surface area, the volume enclosed by the vesicle, and the radius of gyration (the average extension) of the vesicle surface, respectively.

The universality hypothesis is a cornerstone in classifying the critical behavior of diverse systems. It states that a few key attributes such as the spatial dimensionality and the symmetry of the ordering uniquely determine the exponents characterizing the system. For example, seemingly diverse systems such as a fluid at its critical point, a three-dimensional Ising ferromagnet at its Curie point, a binary alloy that is about to order, and a binary fluid mixture that is about to undergo phase separation all have the same critical exponents characterizing their long length scale behavior and are in the same universality class. We show here, that the topology of the surface is such an attribute.

We consider a discretized version of the model on a cubic lattice. The surfaces are constructed by taking elementary plaquettes (squares) and gluing them together such that each edge is shared by exactly two plaquettes. In this case $\chi = c'_2 - c'_1 + c'_0$, where c'_0, c'_1, and c'_2 are the number of vertices, edges, and faces on the vesicle surface, respectively. The area $S = c'_2$ and the enclosed volume V is the number of cubes inside the closed surface. The lattice constant is taken to be a unit length. Recent Monte Carlo simulations (*4, 5*) with a $H = 0$ constraint have indicated that $d_V \simeq d_S \simeq 2 \pm 0.08$. These exponents and the entropy exponent characterizing the number of surfaces of a given area are in excellent agreement with the corresponding exponents of branched polymers (*6*). This result suggests an entropic mechanism that favors tube-like and ramified objects made up of elementary cubes (Fig. 2). Further evidence that the $H = 0$ model is in the branched polymer universality class is provided by analytic and numerical work (7)—on turning off the self avoidance condition, the geometry of the vesicle is found to be identical to that of the free branched polymer. It is commonly believed and probably correct that models with a $H \leq H_o$ constraint (H_o is an arbitrary positive number) are also in the same universality class. In this report, we demonstrate the striking role played by topology in determining the universality class. In particular, we show analytically that the model with unrestricted H is in a different universality class than the constrained H model.

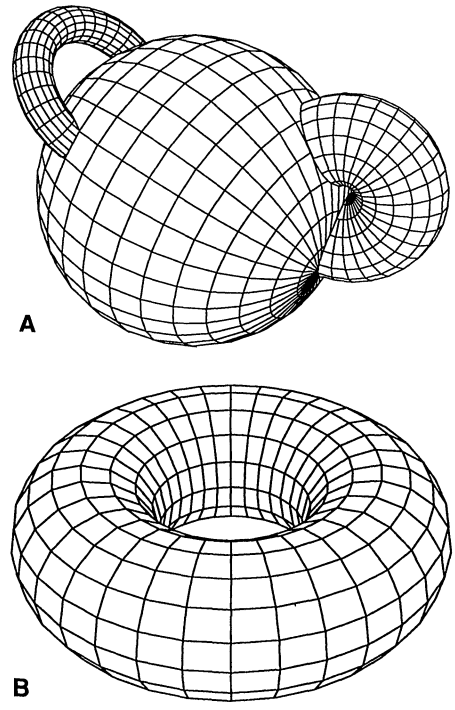

Fig. 1. (**A**) Schematic sketch of a sphere with two handles. Note that an elastic deformation of the surface leaves the number of handles unchanged. (**B**) A donut is equivalent to a sphere with one handle.

In the grand canonical ensemble, the generating function is given by

$$G(K; \bar{p}) = \sum_S{}' K^S e^{\bar{p}V} \qquad (1)$$

where the sum is over the set of three-dimensional vesicles with the constraint that a given plaquette belongs to the surface. K is the fugacity associated with the surface area and $\bar{p}$ denotes the pressure difference between the inside and outside of the vesicle in units of $k_B T$. The sum in Eq. 1 is divergent for any $K > 0$ for $\bar{p} > 0$ since a subset of the

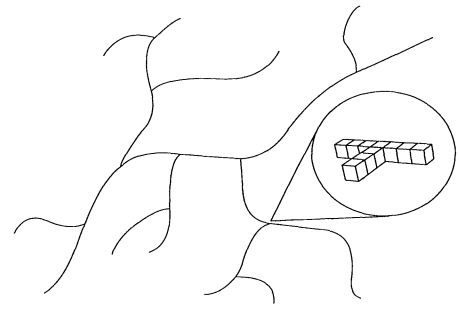

Fig. 2. Schematic sketch of a tubular configuration. The inset shows the microscopic details of cubes glued together such that each edge is shared by at most three cubes.

J. R. Banavar and A. Maritan, Department of Physics and Materials Research Laboratory, The Pennsylvania State University, University Park, PA 16802.
A. Stella, Dipartimento di Fisica, Universita di Bologna, I40126 Bologna, Italy, and Centro Interuniversitario Struttura della Materia, Universita di Padova, Padova 35131, Italy.

*On leave of absence from Dipartimento di Fisica dell' Universitá di Bari and Sezione INFN di Bari, Bari, Italy.

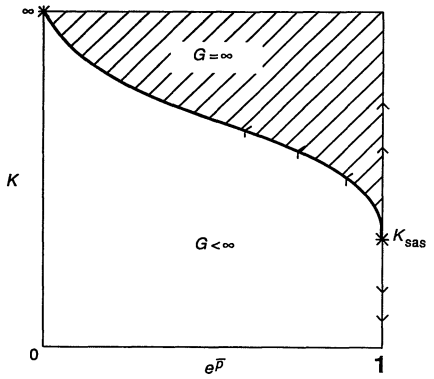

Fig. 3. Schematic phase diagram in the $K - \bar{p}$ plane. The * indicates fixed points, the arrows the renormalization group flows and the critical line separates regions where the generating function $G(K; \bar{p})$ is finite and infinity.

vesicles have $V \propto S^{3/2}$. Thus we restrict ourselves to the deflated regime, that is $\bar{p} \leq 0$ where a non-zero critical fugacity $K_c(\bar{p})$ exists separating finite and infinite values of G (Fig. 3). We now show that the singularity structure for Eq. 1 is identical to that of a gauge model defined by a reduced Hamiltonian

$$H = K \sum_{P} \sum_{\alpha=1}^{n} \prod_{b \in \partial P} s_b^{\alpha}\, \sigma_P + u \sum_{C} \prod_{P \in \partial C} \sigma_P \qquad (2)$$

where P and C denotes a plaquette and cube, respectively and ∂P and ∂C their boundaries, $\mathbf{s}_b$ is an n component vector on the bonds having modulus $\sqrt{n}$ and $\sigma_P = \pm 1$ is an Ising variable residing on a plaquette. The Hamiltonian Eq. 2 is invariant under local gauge transformation $\mathbf{s}_b \to \varepsilon_b \mathbf{s}_b$, $\sigma_P \to \Pi_{b \in \partial P} \varepsilon_b \sigma_P$ with the bond variable $\varepsilon_b = \pm 1$. We will focus on the $n \to 0$ limit. As $u \to \infty$, the second term is maximized by the choice $\sigma_P = 1$ modulo a gauge transformation. In this limit Eq. 2 reduces to a model for a closed, self-avoiding surface with an unrestricted number of handles and is a generalization of the well-known de Gennes self-avoiding walk model (*8*). This limit has been analyzed in detail by Maritan and Stella (*9*). They find that the radius of gyration R and the correlation length ξ have the same singular behavior, where ξ is defined in terms of the plaquette-plaquette correlation function. They also show that the partition function Z and the generating function G are related by

$$\lim_{n \to 0} K \frac{\partial}{\partial K} \frac{\ln Z(K; u = \infty)}{nN} = 3K^2 + G(K; \bar{p} = 0) \qquad (3)$$

where N is the total number of sites of the lattice. It is straightforward to extend their analysis to arbitrary, positive, u by using earlier results of Wegner (*10*) and Kadanoff (*11*). Specifically, the partition function is evaluated by first tracing over the $\mathbf{s}_b$'s and then over the σ_P's. The former leads to closed surfaces denoted by Γ except that there is an additional contribution $\prod_{P \in \Gamma} \sigma_P$. We find that

$$\lim_{n \to 0} K \frac{\partial}{\partial K} \frac{\ln Z(K; u)}{nN} = 3K^2 + G(K; \bar{p} = \ln \tanh u) \qquad (4)$$

The equivalence between Eq. 1 and Eq. 2 allows us to study the vesicle problem by analyzing the gauge model.

We envisage carrying out a decimation of the gauge variables and an unspecified renormalization group scheme on the spin variables. The renormalization group analysis of Eq. 2 simplifies dramatically for the u renormalization, because there is no K contribution in the $n \to 0$ limit. Indeed, the K contribution involves closed surfaces of $\mathbf{s}_b$ and is of order n. The u renormalization can therefore be carried out exactly by considering just the second term on the rhs of Eq. 2. Extending the analysis of Kadanoff (*11*) to three dimensions, we find that decimating with a scale factor b,

$$\bar{p}' = b^3 \bar{p} \qquad (6)$$

Figure 3 shows a phase diagram with the renormalization group flows. There are two fixed points of $\bar{p}$, $\bar{p} = 0$, and $\bar{p} = -\infty$. The renormalization group flows are toward the $\bar{p} = -\infty$ fixed point as long as the external pressure exceeds the internal pressure. This corresponds to the magnitude of this pressure difference growing as the vesicle is considered at larger length scales. With Eq. 5, a crossover scaling analysis for the radius of gyration of the surface R yields for an arbitrary scale factor b, $R(\delta K, \bar{p}) = bR(b^{d_S}\delta K, b^3 \bar{p})$ where $\delta K = K - K_c(\bar{p} = 0)$. Setting $\delta K = 0$, $R(0, \bar{p}) = bR(0, b^3\bar{p}) \sim \bar{p}^{-1/3}$. Since $\bar{p}$ is conjugate to the volume of the vesicle (inversely proportional to the volume of the vesicle), at the unstable fixed point $\bar{p} = 0$ the volume V scales as R^3 indicating that $d_V \equiv 3$. This result (while intuitively pleasing) is at odds with the $d_V = 2$ result found for vesicles with a restricted number of handles (*4, 5*). Thus the universality class of vesicles depends on the topological characteristics.

It is important to note that different exponents would be obtained depending on whether the vesicles are studied in a microcanonical ensemble holding the surface area or the volume enclosed constant. The former case should yield $d_V = 3$, whereas the latter would be characterized by $d_V = 2$ when $\bar{p} = 0$. The simulations (*4, 5*) yielding $d_V = 2$ correspond to the former situation but with no handles.

We alert the reader that our analysis has been carried out in the $n \to 0$ limit rather than first treating arbitrary n and then letting $n \to 0$. It turns out that all approximate renormalization group schemes involving a finite number of couplings validate the correctness of this approach. Further evidence for its validity is provided by a recent analysis (*12*) that used a similar approach of the behavior of two-dimensional vesicles in the deflated regime, for which excellent agreement has been found with the previous work of Fisher and co-workers (*13*).

At $\bar{p} = 0$, the elucidation of d_S remains a challenge. The condition $d_S = 3$ would correspond to a space-filling surface while $d_S = 2$ could represent a flat surface. Earlier approximate work based on the Flory approach (*14*) and the intersection of a self-avoiding surface with a plane (*15*) have lead to estimates of $d_S \approx 7/3$.

We now turn to some exact inequalities which provide physical insight into the role played by topology on the vesicle geometry. These inequalities may be derived by using the earlier definition of $\chi = c_2' - c_1' + c_0'$ and $-c_3 + c_2 - c_1 + c_0 = \chi/2$, where c_3 ($\equiv V$), c_2, c_1, and c_0 are the total number of cubes, plaquettes, edges, and vertices in the vesicle. Combining these two equalities, after some manipulations, we find $c_3 = c_2'/4 + (H - 1)/2 + c_1^{\,i} - c_0^{\,i}$ where the superscript i refers to an internal (not on the surface) edge or vertex. Since $c_1^{\,i} \geq c_0^{\,i}$,

$$V \geq \frac{S}{4} + \frac{H - 1}{2} \qquad (6)$$

with the equality holding only when $c_1^{\,i} = c_0^{\,i} \equiv 0$, that is, for branched or tubular configurations constructed by gluing cubes together such that each edge is shared by at most three cubes (Fig. 2). Since the branched polymer configurations (BP) are a subset of all allowed configurations and $\bar{p} \leq 0$, from Eqs. 6 and 1 we find

$$\sum_{\mathrm{BP}}{}' (K^4 e^{\bar{p}})^{V + 1/2} K^{-2H} \leq e^{\bar{p}/2} G \leq \sum_{S}{}' (K^4 e^{\bar{p}})^{S/4} e^{H\bar{p}/2} \qquad (7)$$

Thus $K_c(\bar{p}) \sim e^{-\bar{p}/4}$ as $\bar{p} \to -\infty$. In this limit, $\langle V \rangle \sim \langle S \rangle/4$ indicating that the branched polymer configurations are dominant in the deflated regime. Further, the number of handles H are coupled to $\bar{p}$. As $\bar{p} \to -\infty$, for $K < K_c(\bar{p})$ assuming that there is only one transition, we can show exactly that

$$\langle H \rangle = \frac{1}{G} \sum_{S}{}' K^S e^{\bar{p}V} H \to 0 \qquad (8)$$

A plausible scenario emerges from the above results: the entropy gained by the

presence of handles is more significant when $d_V = 3$ compared to $d_V = 2$. The effect of a deflating pressure is to collapse the vesicle, thereby reducing d_V from 3 to 2. In this deflated regime, it does not pay to continue having the handles. The minimization of the volume accompanied by the divergence of the average surface area as one approaches the critical line favors the breaking up of handles into simpler topologies. In the restricted topology case, the handles are excluded or constrained. It is intriguing that this restriction plays a role similar to that of a deflating pressure leading to the collapsed limit. Our results suggest that even for a fluid membrane, in the absence of a pressure imbalance, the universality class may depend on whether there are restrictions on the number of handles or not.

Why should vesicles with unrestricted handles be fatter ($d_V = 3$) than those with restrictions? A possible mechanism for gaining entropy compared to the tubular configuration of Fig. 2 could be to have a proliferation of fat donut-like handles with very small holes (the baker's nightmare), the small holes can then be placed in many locations leading to a large entropy.

The difference between surfaces with restricted and unrestricted handles is further underscored by the fact that in the absence of self-avoidance and any interaction, the former remains well defined whereas the latter is characterized by an entropy that is not extensive (*16*) and is therefore ill-defined as a statistical mechanics model. The self-avoidance interaction is usually irrelevant above the upper critical dimension. In the case of unrestricted handles, this probably is not the case since the model needs a regulator to be well defined.

REFERENCES AND NOTES

1. See, for example, D. R. Nelson, in *Statistical Mechanics of Membranes and Interfaces*, D. R. Nelson, T. Piran, S. Weinberg, Eds. (World Scientific, Singapore, 1989); F. F. Abraham and D. R. Nelson, *Science* **249**, 393 (1990).
2. A. M. Polyakov, *Gauge Fields and Strings* (Harwood Academic, New York, 1982).
3. A self-avoiding, closed surface in three dimensions is orientable, see, for example, H. S. M. Coxeter, *Regular Complex Polytopes* (Cambridge Univ. Press, New York, 1974); *Introduction to Geometry* (Wiley, New York, 1969).
4. U. Glaus and T. L. Einstein, New York, *J. Phys.* **A20**, L105 (1987); U. Glaus, *J. Stat. Phys.* 50, 1141 (1988).
5. J. O'Connell *et al.*, in preparation.
6. G. Parisi and N. Sourlas, *Phys. Rev. Lett.* **56**, 871 (1981).
7. B. Durhuus, T. Jonsson, J. Frohlich, *Nucl. Phys.* **B240**, 453 (1984)
8. P. G. de Gennes, *Scaling Concepts in Polymer Physics* (Cornell Univ. Press, Ithaca, 1979).
9. A. Maritan and A. L. Stella, *Nucl. Phys.* **B280**, 561 (1982).
10. F. J. Wegner, *J. Math. Phys.* **12**, 2259 (1971).
11. L. P. Kadanoff, *Rev. Mod. Phys.* **59**, 267 (1977).
12. J. R. Banavar, A. Maritan, A. L. Stella, *Phys. Rev. A*, in press.
13. S. Leibler *et al.*, *Phys. Rev. Lett.* **59**, 1989 (1987); M. E. Fisher, *Physica* **38D**, 112 (1989); C. J. Camacho and M. E. Fisher, *Phys. Rev. Lett.* **65**, 9 (1990).
14. A. Maritan and A. L. Stella, *Phys. Rev. Lett.* **53**, 123 (1984).
15. P. Pfeifer, U. Welz, H. Wippermann, *Chem. Phys. Lett.* **113**, 535 (1985).
16. T. Eguchi and H. Kawai, *Phys. Lett.* **110B**, 143 (1982).

17. We are grateful to M. Fisher and B. Harris for stimulating discussions and many helpful suggestions. We are indebted to J. Maynard for drawing the figures for us with DataScript Scientific Software. The work at Penn State was supported by grants from the NSF, NASA, and the Petroleum Research Fund administered by the American Chemical Society.

18 December 1990; accepted 13 March 1991

Ultradeep (>300 Kilometers) Ultramafic Xenoliths: Petrological Evidence from the Transition Zone

VIOLAINE SAUTTER, STEPHEN E. HAGGERTY, STEPHEN FIELD

The seismologically delineated transition zone, at depths between 400 and 670 kilometers, is a fundamental discontinuity in the earth that separates the upper mantle from the lower mantle. Xenoliths from within or close to the transition zone are dominated by pyropic garnet and associated pyroxene or mineralogically heterogeneous garnet lherzolite. These xenoliths show evidence for the high-pressure (90 to 120 kilobars) transformation of pyroxene to a solid solution of pyroxene in garnet (majorite) and silicon in octahedral coordination; low-pressure (less than 80 kilobars) exsolution of clinopyroxene or orthopyroxene from the original majorite is preserved. Although mineral modes and rock proportions below the transition zone and the relative amount of eclogite present cannot be accurately assessed from the xenoliths, it is likely that both majorite and β-spinel help produce the observed seismic gradient of the transition zone.

WHETHER THE DISCONTINUITY AT a depth of 400 km reflects an isochemical phase change from olivine to β-spinel (model 1) or a chemical change related to pyroxene dissolution in garnet (model 2) is controversial; a related issue is whether the mantle is homogeneous (*1*) or is stratified as a result of the transformation of peridotite at a depth of 400 km into piclogite [olivine eclogite (*2, 3*), model 2]. Because of the lack of natural samples, mineral assemblages and the mantle composition between depths of 200 km and the transition zone at 400 to 670 km have previously been indirectly inferred either from comparisons of elastic moduli of silicates and oxides with predictions from seismic velocity data or from results of high-pressure experimental investigations (*4–7*). Recently, however, deep mantle xenoliths have been identified from the vicinity of this discontinuity (*8*). These rocks were transported to the crust by an eruptive kimberlite at Jagersfontein, located close to the southeast edge of the Kaapvaal craton in South Africa. In this report we describe two additional samples from this pipe that help to characterize the relation between pyroxene and garnet and the compositional variation of this part of the mantle.

The mantle xenoliths that we described earlier from this kimberlite contain a close association of ultramafic pyrope-rich garnet [69 to 73% pyrope (on a mole basis), 15 to 20% almandine, and 11 to 12% grossular] substituted by Cr (up to 2% by weight Cr_2O_3) and ternary clinopyroxene (20% jadeite, 74% diopside, and 6% enstatite). The clinopyroxene forms either oriented <111> rods in the garnet host or is present as discrete crystals attached to garnet in a cuspate and sealed grain-boundary contact. Both textural types of pyroxene exsolved from garnet as a result of pressure release at a depth of 100 to 150 km from the original depth of 300 to 400 km. When the clinopyroxene component is recombined with the host garnets' composition, a garnet with excess Si is produced; the Si/Al atomic ratio of these garnets is similar to that of garnets in diamond inclusions from the Jagersfontein (*9*) and Monastary (*10*) diamond mines in South Africa and Sao Luiz in Brazil (*11*). This excess Si is in octahedral coordination (Si^{VI}), is associated with an Al^{VI} deficit (unbalanced by Cr and Ti), and is typical of the chemical signature of a pyroxene component dissolved in the garnet structure (*12*).

We have processed 324 samples (mostly in the range 0.5 to 3 cm in diameter) from Jagersfontein, of which about 10% contain

V. Sautter, Laboratoire de Géophysique et de Géodynamique Interne, Université de Paris–Sud, 91405 Orsay CEDEX, France.
S. E. Haggerty, Department of Geology, University of Massachusetts, Amherst, MA 01003.
S. Field, Department of Geology, Stockton State College, Pomona, NJ 08240.